Supplementary Figures.

Apurinic endonuclease-1 preserves neural genome integrity to maintain homeostasis, thermoregulation and prevent brain tumors.

Lavinia C. Dumitrache[1], Mikio Shimada[1, 2], Susanna M. Downing[1], Young Don Kwak[1], Yang Li[1], Jennifer L. Illuzzi[3], Helen R. Russell[1], David M. Wilson 3[rd, 3] & Peter J. McKinnon[1,4,5].

[1]Department of Genetics, St. Jude Children's Research Hospital, Memphis, TN, USA and [2]present address: Tokyo Institute of Technology, Japan, [3]Laboratory of Molecular Gerontology, National Institute on Aging, Intramural Research Program, National Institutes of Health, Baltimore, MD, USA, [4]St Jude Graduate School of Biomedical Sciences.

[5]To whom correspondence should be addressed: peter.mckinnon@stjude.org

This Supplementary data set includes:

- Supplementary text
- Fig. S1 to S9
- Table S1
- References

www.pnas.org/cgi/doi/10.1073/pnas.1809682115

Materials and Methods

Generation of *Ape1* conditional knockout mouse.

Proximal to Exon 1 of *Ape1* there is an initiating exon of a different gene, *Osgep*, which transcribes in the opposite direction. In addition, exons 4 and 5 of Ape1 overlap the untranslated 3' end of another gene, *Tmem55b*. The targeting strategy introduced LoxP sites spanning exons 2 and 3 of *Ape1* thus deleting the initiating ATG and the second coding exon, using recombineering (Liu et al., 2003) to initially introduce a single LoxP site between exons 3 and 4. Then, a neomycin selection cassette flanked by Frt sites and a single LoxP site was inserted between exon 1 and 2. The targeting construct was linearized and electroporated into W9.5 embryonic stem cells (ES cells), and following G418 selection the clones were screened by southern blotting using 3' and 5' probes which hybridized outside the target construct region. Positive clones with normal karyotypes were injected into E3.5 blastocysts to generate chimeric mice. The male chimeras were bred with C57BL/6 females to establish germline transmission of the targeted *Ape1* allele and further interbred with Flp recombinase mice (JAX #003800:B6; SJL-TG(ACTFLPE)9205 DYM/J) to remove the neomycin cassette resulting in a conditional floxed *Ape1* allele without a selection cassette containing eukaryotic promoter elements.

To inactivate *Ape1* in the nervous system, we bred $Ape1^{LoxP}$ mice with Nes-cre (B6.Cg-Tg(Nes-cre)1Kil/J; JAX#003771). *Sox2-cre* (JAX #004783; Tg(Sox2-cre)1Amc) was used to delete *Ape1* throughout the embryo (but not the placenta) to generate an *Ape1-null* ($Ape1^{-/-}$) mouse. CreTM (JAX #004682; B6.Cg-Tg(CAG-cre/Esr1)5Amc/J), in which cre driven from an actin promoter with a CMV enhancer

can be induced by taxmoxifen were used as a source for generation of E14 primary mouse embryonic fibroblasts. Generation of $p53^{LoxP}$, $Xrcc1^{LoxP}$, $Brca2^{LoxP}$ mice has been described previously (Frappart et al., 2007, Lee et al., 2009). Confirmation of correct genotypes was done via PCR using gene specific primer sets. All animal experiments were carried out according to NIH regulations and were approved by the SJCRH Animal Care and Use Committee.

Body temperature measurement. To collect the body temperature, IPTT-300 temperature transponder (BMDS, Bio Meduc Data Systems) was implanted subcutaneously into 6-weeks old WT and $Ape1^{Nes\text{-}cre}$ mice. Temperatures were collected for 5 consecutive days, twice a day (at 8am and 12pm), either while mice were on the heating pad (37^{o}C) or 90 minutes after the mice were maintained at (20^{o}C). Three mice per genotype were used for this experiment.

Histology and immunodetection. For cryosection, mice underwent transcardial perfusion with 4% (w/v) buffered paraformaldehyde (PFA) and embryos were drop-fixed in 4% PFA. After cryoprotection in buffered 25% sucrose (w/v) solution; brains and embryos were embedded in Tissue-Tek OCT compound (Sakura), and sectioned at 9μm using a CM3050S cryostat (Leica). For paraffin sections, brains were fixed in 10% buffered formalin (vol/vol), embedded in paraffin and section at 5μm using an HM325 microtome (Microm).

NISSL and hematoxylin and eosin (HE) stainings were performed according to standard procedures. Prior immunodetection, sections were subject to antigen

retrieval according to the manufacturers directions (HistoVT One, Nacalai Tesque). For immunodetection, the following antibodies (in alphabetical order) were used: Ape1 (1:500, Novus, NB100-101), Brn2 (1:200, Gene-Tex, GTX114650), CNPase (1:500, Sigma, C5922), Calbindin (1:500, Sigma, C9848), CAR8 (1:500, Novus, NB100-74382), c-Fos (1:250, Novus, NB100-91772), Egr2 (1:500, Novus, NB110-59723), GFAP (1:500, Sigma, G3893), γH2AX (rabbit, Ser-139, 1:500, Cell Signaling, 2577, and mouse, 1:500, Millipore, 05-636), IBA1 (1:500, Novus, NB100-1028), phospho KAP-1 (S824) (1:500, Bethyl, A300-767A), Myelin Basic Protein (1:500, Abcam, ab40390), MAP2 (1:500, Abcam, ab32454), MATH1 (1:1000, Abcam, ab27667), NeuN (1:500, Chemicon, MAB377), Olig2 (1:500, Millipore, AB9610), Parvalbumin (1:500, Millipore, MAB1572), Pax2 (1:500, Zymed, 71-6000); PCNA (1:500, Santa Cruz, SC-56), myelin PLP (1:1000, Abcam, ab105784), Satb2 (1:50, Abcam, ab51502), Sox10 (1:250, Abcam, ab155279), Tbr1 (1:100, Abcam, ab31940), TPH2 (1:500, Abcam, ab121013), Vglut3 (1:100, Novus, NBP2-59331). FITC- and Cy3-conjugated secondary antibodies (Jackson Immunologicals) were used and counterstained with 4'6-diamidino-2-phenylindole (DAPI; Vector Laboratories). For colorimetric immunodetection, the standard protocol was performed using biotinylated secondary antibody and avidin-biotin complex (Vectastain Elite kit, Vector labs) and VIP substrate kit (Vector Labs) according to the manufacturer's protocol. Sections were counterstained with methyl green (Vector Labs), dehydrated and mounted in DPX (Electron Microscopy Sciences).

Apoptosis was measured by TUNEL assay using Apoptag (Millipore) according to the manufacturer's protocol. Sections were counterstained with

propidium iodide (PI) in mounting medium (Vector Laboratories). At least three independent tissue samples from each genotype was used for all experiments and analyses.

Primary astrocytes and immunofluorescence. Primary astrocytes were prepared from P3 mouse brains as described previously (Katyal et al, 2007) using Dulbecco's modified Eagle's medium and Ham's nutrient mixture F-12 (1:1 DMEM/F12, Gibco-BRL) supplemented with 10% fetal bovine serum (v/v), 1x glutamax, 100 U/ml penicillin, 100mg/ml streptomycin and 20 ng/ml epidermal growth factor (EGF; Millipore). Primary astrocytes were maintained in Primaria T-25 tissue culture flasks (Falcon) at 37°C in a humidified CO_2-regulated (5%) incubator.

For immunofluorescence, astrocytes were grown on CC2 treated glass chamber slides (LAB-TEK, Thermo Fisher Scientific) and fixed with 4% PFA solution. Cells were stained with primary antibodies (described above), Alexa Fluor 488/555-conjugated secondary antibodies (Life Technologies) and counterstained with DAPI (Vector Laboratories). All experiments were performed in triplicate.

APE1 enzymatic assay.

Primary embryonic (E14) fibroblasts were isolated from $Ape1^{CreTM}$ mice. APE1 inactivation was done using 1μM tamoxifen for 48-72h prior to cell lysis. Total cell extracts were prepared using 1x RIPA buffer with 1× Halt protease inhibitor cocktail (Pierce). Cells were lysed for 30min on ice, and the solution was centrifuged for

15min at 18,000g at 4°C. Protein concentrations were determined using either a Bradford assay (BioRad) or the BCA protein assay kit (Thermo Scientific).

AP site incision assays were performed using a double-stranded oligonucleotide substrate, in which one strand harbored an abasic site analog, tetrahydrofuran (THF) (Illuzzi et al., 2017). Whole cell extracts with 1x reaction buffer (50mM Tris, pH 7.5, 25mM NaCl, 1mM $MgCl_2$, 1mM DTT, 0.01% Tween-20) and 1pmol of 5'-[^{32}P]-labeled double-stranded DNA, were incubated with the labeled strand harboring the AP site analog tetrahydrofuran (THF), in 10 µl reactions. Reactions were incubated at 37°C for 15 min, before an equal volume of stop buffer was added (90% formamide, 20mM EDTA). Reactions were heated to 95°C for 10min before separation on a 20% polyacrylamide-urea denaturing gel. The substrate and product bands were visualized and quantified by a Typhoon Trio+ Variable model Imager (Amersham Bioscience/GE Healthcare) using the ImageQuant software to determine percent conversion.

AP site detection assay. Primary astrocytes were grown on CC2 treated glass chamber slides (LAB-TEK, Thermo Fisher Scientific) and AP-site Assay Kit (Abcam, ab133076) was used according to the manufacturer's protocol. Epigallocatechin Gallate (EGCG) (1:200) included in the kit was used as a positive control.

Proliferation assay. Passage 2 primary astrocytes were seeded onto 24-well plates ($5x10^3$ cells per well). Cells were trypsinized and counted every 3 days and re-

seeded at the same density ($5x10^3$ cells/well). Seeding and counting were repeated until passage 6. The experiment was performed in triplicate using multiple clones.

Cell treatments and survival assay. Passage 3 primary astrocytes were grown onto 24-well plates (10^4 cells per well) in day 0. Next day, day 1, cells were treated with methylmethane sulphonate (MMS, Sigma) (100μM, 200μM, 400μM), hydrogen peroxide (H_2O_2, Thermo Fisher) (50μM and 100μM), Cis-Diammine platinum (II) (Cisplatin, Sigma) (0.2μM, 0.4μM, 0.8μM) or γ-irradiation (10Gy and 20Gy). Cells were counted on day 4. The experiment was performed in triplicate using multiple clones.

Fluorescence in situ hybridization (FISH) analysis. Cryo or paraffin sections containing mouse brain tumor tissue specimens were analyzed for Ptch1 and MycN deletion/amplification, using a standard FISH protocol: 200 nuclei from each sample were scored.

Alkaline comet assay. Cells were treated with 150μM H_2O_2 (Thermo Fisher) on ice for 5 min, methylmethane sulphonate (MMS, Sigma) for 10min at 0.2mg/ml at 37° C, 14μM camptothecin (CPT, Calbiochem) at 37°C for 30min or 60min, or γ-irradiation (20Gy). Alkaline comet assay was performed as previously described (Katyal et al, 2007). Comets were stained with SYBR Green (1:10,000 in 0.4 M Tris-HCl, pH7.5) for 10 min, and then analyzed using the Comet Assay IV system (Perceptive

Instruments) with Axioskop2 and microscope (Carl Zeiss) at x200 magnification. Experiments were triplicated, and at least 100 comets/experiment were counted.

Western blotting. Mouse tissues were harvested and extracted in RIPA buffer (0.1M Tris HCl ph7.5, 0.5M NaCl, 0.05M EDTA, 1% Triton X-100, 1% SDS, 1% sodium deoxycholate) with a protease inhibitor cocktail (Roche). Western blot analysis was performed as described previously (Shimada et al, 2015) and primary antibody used was anti-Ape1 (1:500, Novus, NB100-101). Antibody binding was identified using Amersham ECL western blotting detection reagent (GE healthcare life sciences). Ponceau S staining was used to confirm equal protein loading.

***In situ* cell counts.** Sections from three mouse brains for each genotype were analyzed. All statistics were calculated using unpaired student's t-test.

Kainic acid treatment. P5 mice were intraperitoneally injected with kainic acid monohydrate (KA) (Sigma, K0250) at a dose of 1.5mg/Kg. After 2 hours, mice were euthanized with CO_2, according to NIH regulations and with approval from the SJCRH Animal Care and Use Committee, and hippocampi were collected either to generate cryosections for immunofluorescence analysis or for further microarray analysis.

Microarray analysis. P5 mice were euthanatized using CO2. Total RNA was extracted from the hippocampus using TRIzol (Ambion, Life Technologies). RNA

was evaluated for quality control using Agilent 2100 Bioanalyzer (RNA 6000 Nano assay) and submitted for microarray analysis using Mouse Gene 2.0 ST platform.

For P5 hippocampus, values were returned and Robust Multi-array Average (RMA) normalized then further processed using the batch effect correction tool in ParTek Genomics Suite version 6.6. Fold Change (FC) was calculated after normalization using means of control untreated samples compared with control two hours post kainic acid treatment. Heatmaps were generated in R with normalized, batch corrected microarray data and utilize row z-scores for scaling. Probes were selected based on FC cut off levels (either >1.4 or >1.5) between WT and WT +KA 2 hours post-treatment, using a p-value<0.05 from a student t-test.

Chromatin immunoprecipitation (ChIP). WT and *Ape1*$^{Nes\text{-}cre}$ P5 mice were injected with kainic acid monohydrate (KA) (Sigma, K0250), and 90 minutes later hippocampi were collected. Tissue extract was crosslinked with 1% formaldehyde for 12 min and the reaction was stopped with 0.25M Glycine for 5 min at room temperature. Samples were then washed with ice cold PBS containing 1x protease inhibitor cocktail (Sigma, P8340). Chromatin was extracted in lysis buffer (0.25% Triton X-100, 1mM EDTA pH8.0, 140mM NaCl, 50mM HEPES pH7.9, 10% Glycerol, and 0.5% NP-40), washed (1mM EDTA pH8.0, 200mM NaCl, 10mM Tris HCl pH8.0, and 0.5mM EGTA pH 8.0) and then sheared in 0.1% SDS, 1mM EDTA pH8.0 and 10mM Tris HCl pH8.0 to generate DNA fragments of 200-500bp using a Covaris M220 sonicator (Covaris). c-Jun antibody (5µg, Abcam, #ab31419) and Magna ChIP™ Protein A+G Magnetic Beads (20µl, Millipore, #16-663) were added to the chromatin and incubated overnight at 4°C. Beads

were washed with low salt buffer (0.1% SDS, 1% Triton X-100, 2mM EDTA, 20mM Tris HCl pH8.0 and 150mM NaCl), high salt ChIP wash buffer (0.1% SDS, 1% Triton X-100, 2mM EDTA, 20mM Tris HCl pH8.0 and 500mM NaCl), LiCl ChIP wash buffer (1mM EDTA, 10mM Tris HCl pH8.0, 250mM LiCl, 1% NP-40, and 1% sodium deoxycholate), and TE buffer (1% SDS, 1mM EDTA and 10mM Tris HCl pH8.0). Immunoprecipitated DNA was eluted using elution buffer (0.1 M $NaHCO_3$/1% SDS) and reversion was performed by adding 4µl of 5M NaCl per IP at 65°C overnight. Immunoprecipitated DNA was incubated with proteinase K at 37°C for 2hrs, and DNA was isolated using phenol-chloroform protocol and analyzed via quantitative PCR (Applied Biosystems 7500 Real Time PCR System). Primers used for PCR amplification of precipitated DNA are as follows: Egr2, 5' CTGCCATTAGTAGAGGCTCAGG (forward), 5' GTTCTACAGCCGTCATCCTGG (reverse), Npas4, 5' AGCTGCTGCCAGGCTATTTT (forward), 5' GCTCTGTATGCCCCCAATGT (reverse) and JunB, 5' ATGACCCCAACCTTTGCTAGAT (forward), 5' CCCATAAGTGGAAAAGGGAAGGA (reverse).

REFERENCES.

1. Frappart PO, Lee Y, Lamont J, McKinnon PJ (2007) BRCA2 is required for neurogenesis and suppression of medulloblastoma. EMBO J 26: 2732-42
2. Iluzzi JL, McNeill DR, Bastian P, Brenerman B, Wersto R, Russell HR, Bunz F, McKinnon PJ, Becker KG, Wilson DM, 3rd (2017) Tumor-associated APE1 variant exhibits reduced complementation efficiency but does not promote cancer cell phenotypes. Environ Mol Mutagen 58: 84-98

3. Katyal S, el-Khamisy SF, Russell HR, Li Y, Ju L, Caldecott KW, McKinnon PJ (2007) TDP1 facilitates chromosomal single-strand break repair in neurons and is neuroprotective in vivo. EMBO J 26: 4720-31
4. Lee Y, Katyal S, Li Y, El-Khamisy SF, Russell HR, Caldecott KW, McKinnon PJ (2009) The genesis of cerebellar interneurons and the prevention of neural DNA damage require XRCC1. Nat Neurosci 12: 973-80
5. Liu P, Jenkins NA, Copeland NG (2003) A highly efficient recombineering-based method for generating conditional knockout mutations. Genome Res 13: 476-84
6. Shimada M, Dumitrache LC, Russell HR, McKinnon PJ (2015) Polynucleotide kinase-phosphatase enables neurogenesis via multiple DNA repair pathways to maintain genome stability. EMBO J 34: 2465-80

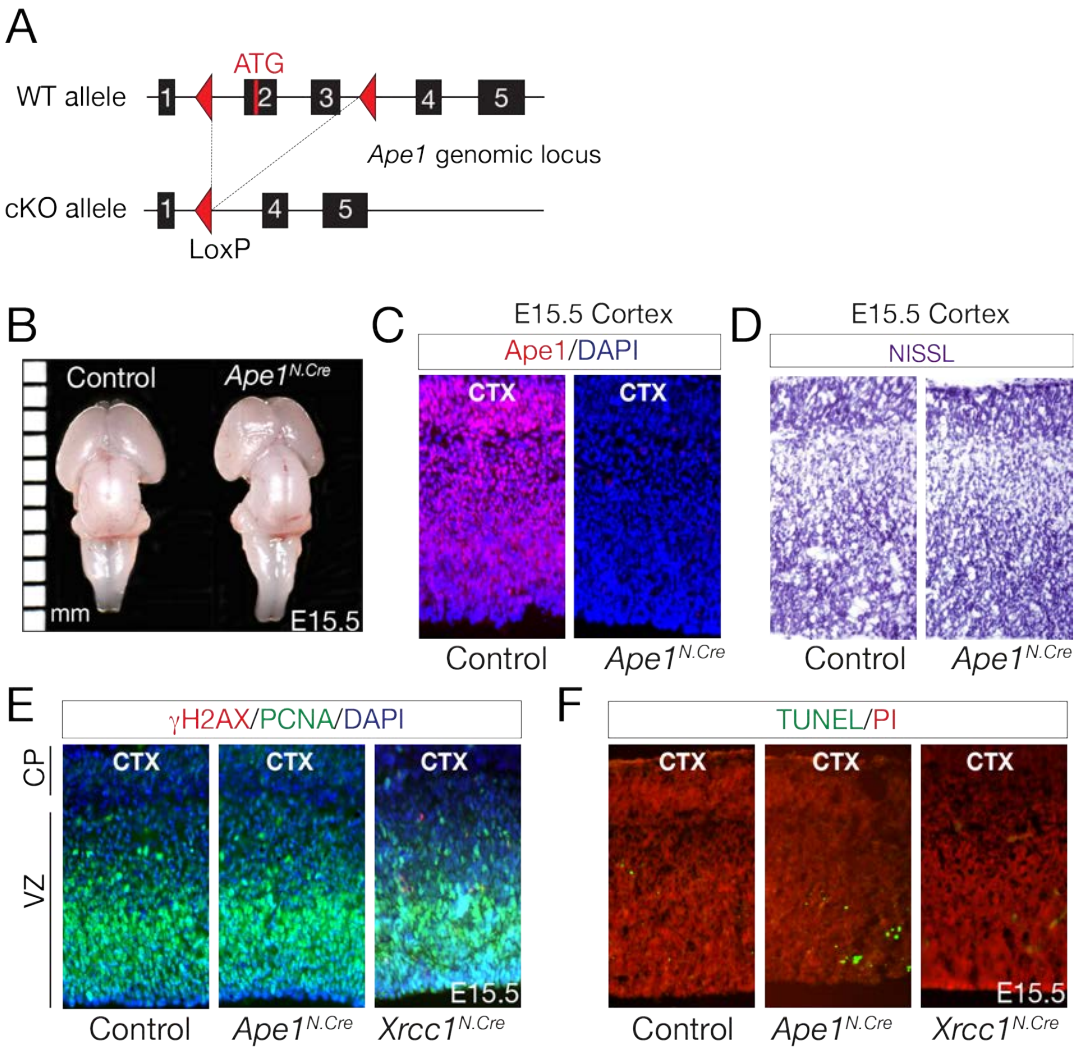

Supplementary Figure 1: Inactivation of APE1 throughout the nervous system does not affect neurogenesis.

A mouse conditional *Ape1* allele was constructed by placing *LoxP* sites flanking exon 2 and 3 to generate an out-of-frame message after cre-mediated deletion, causing loss of APE1 function. (B) During development no perturbations associated with APE1 loss were observed. (C) *Ape1*$^{Nes\text{-}cre}$ embryos developed normally, despite full inactivation of APE1 as shown by a lack of detectable protein at E15.5. (D) The

histology of all regions of the nervous system was normal as judged by Nissl staining. The embryo has normal patterns of proliferation and no elevated DNA damage as detected using PCNA and γH2AX immunostaining, (E) nor was apoptosis elevated as judged by TUNEL staining (F). These findings were consistent in embryos between E13-E18 (i.e. until birth).

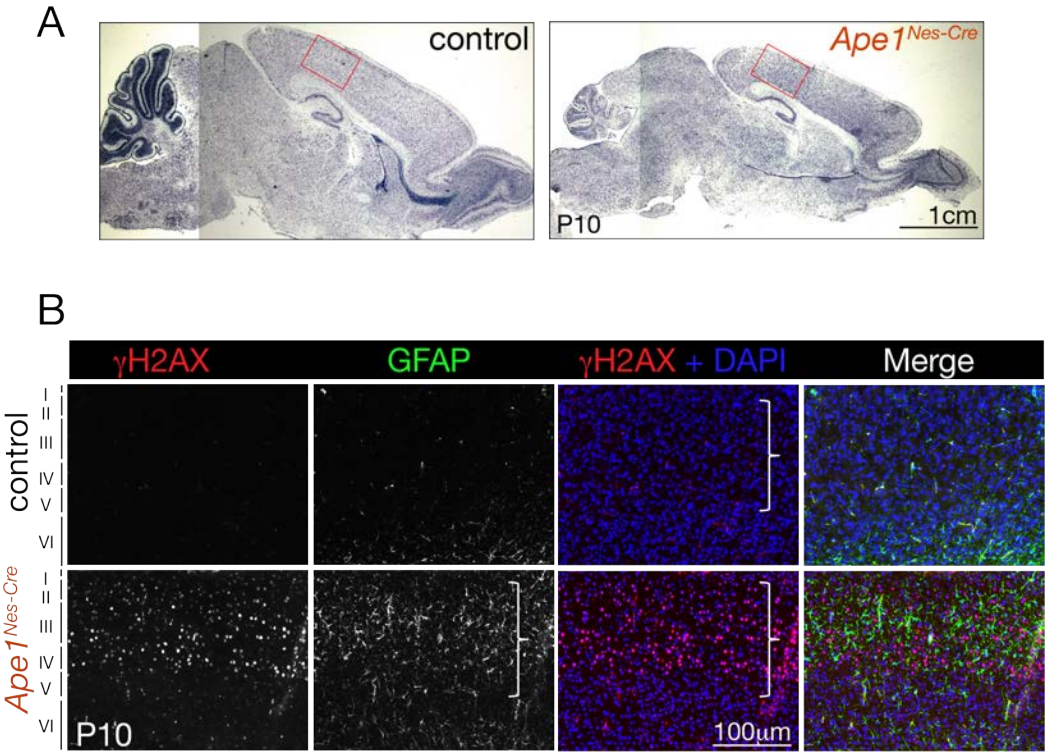

Supplementary Figure 2: DNA damage is concentrated in the upper-cortical layers after neural APE1 inactivation.

Analysis of the postnatal *Ape1*$^{Nes\text{-}cre}$ brain showed that an early reduction in size of the cortex (boxed area in "A") was apparent. The cerebellum also shows a marked developmental defect. (B) Increased DNA damage as determined using γH2AX is present in the *Ape1* mutant tissue, but was absent from control brain (indicated by white brackets). The γH2AX signal was increased in the upper cortical layers (layers II-IV) at P10. Glial fibrillary associated protein (GFAP) is also elevated, and its immunostaining overlaps the region of increased DNA damage. This suggests the elevated DNA strand breaks promote gliosis, and indicates perturbed neural homeostasis associated with the increased DNA damage in the *Ape1* mutant tissue.

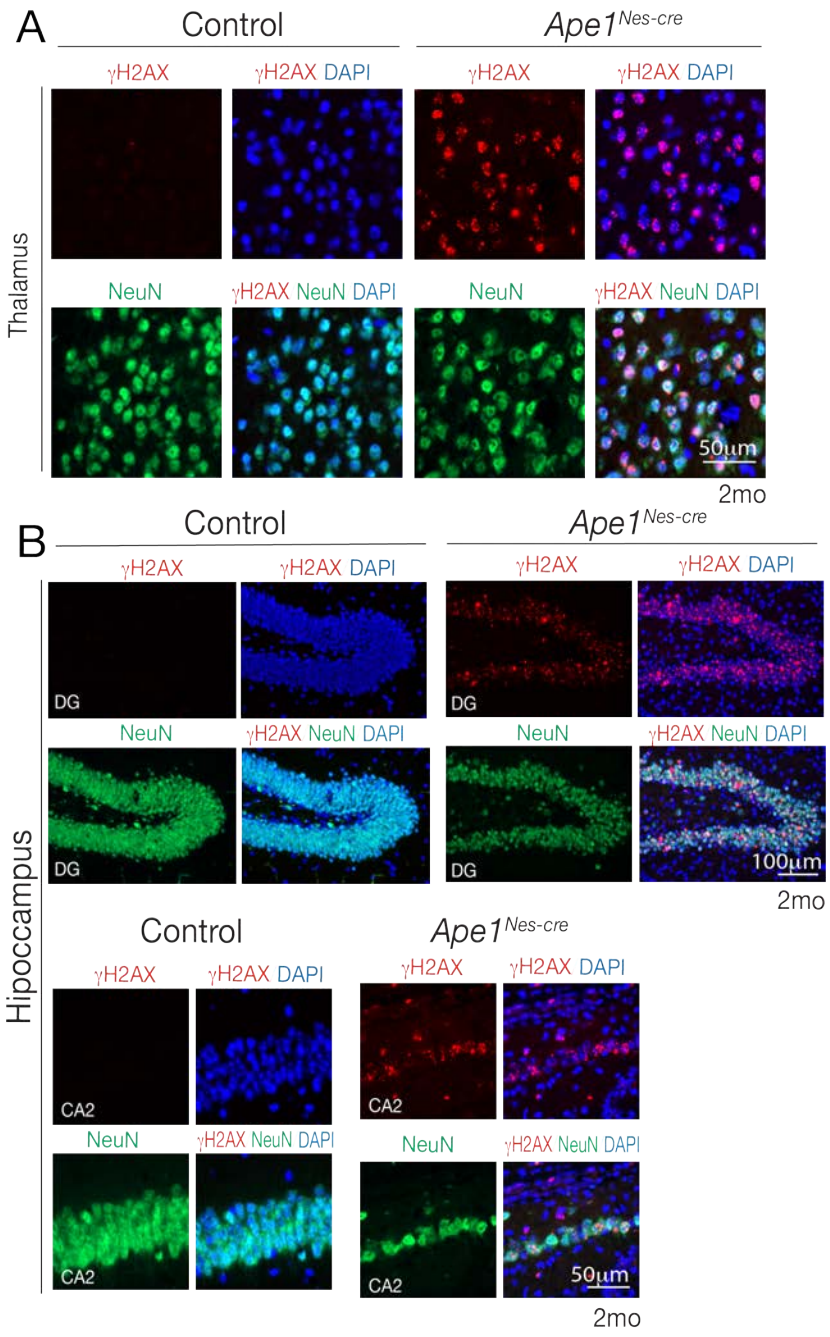

Supplementary Figure 3: DNA damage resulting from inactivation of APE1 is widespread in the postnatal brain.

DNA damage occurrence as determined using γH2AX immunostaining was widespread throughout the brain at 2 months of age. However, areas such as the

thalamus (A) and hippocampus (B) showed very elevated levels of damage. Despite these levels of DNA damage at 2 months of age, cellularity as shown by the mature neuronal marker NeuN was intact. Little to no immunoreactivity for γH2AX was observed in control tissue. DG is the dentate gyrus and CA2 is the cornu ammonis region 2.

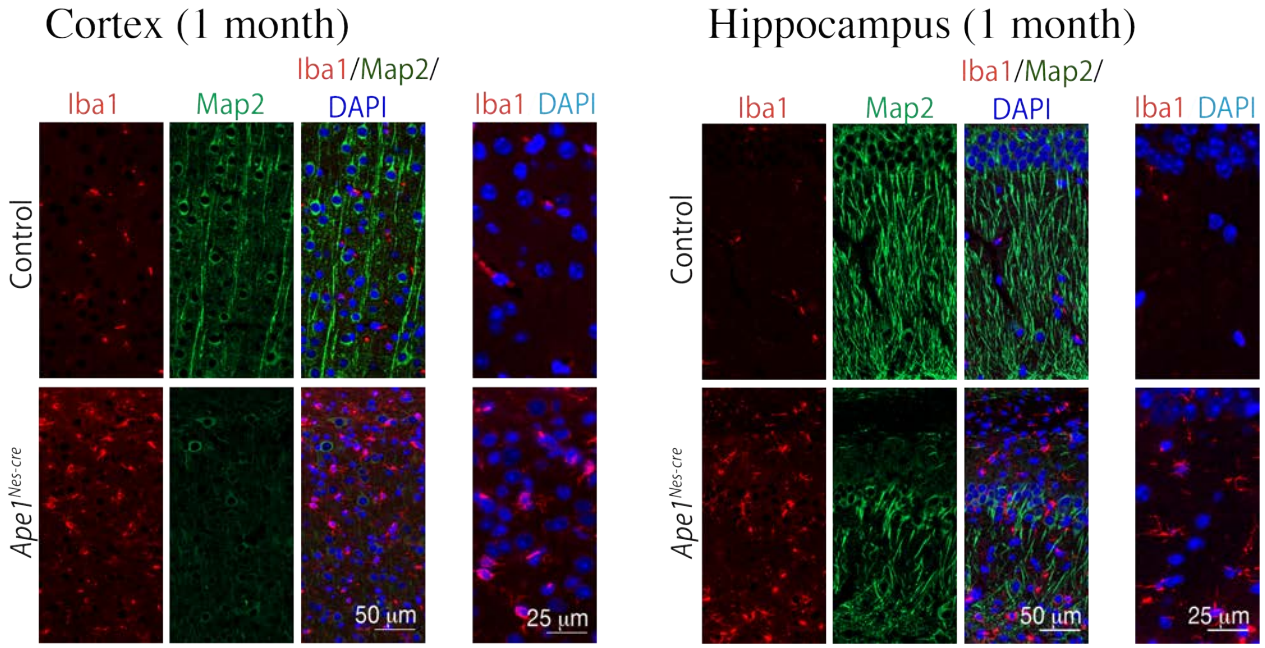

Supplementary Figure 4: Loss of APE1 results in inflammation in the nervous system.

The inflammatory marker Iba1 (ionized calcium-binding adapter molecule 1, which is localized to microglia) was elevated in the *Ape1*$^{Nes\text{-}cre}$ brain through the 1 month old cortex and hippocampus. In these regions of inflammation the levels of the neuronal cytoskeletal marker MAP2 (microtubule-associated protein 2) was also reduced. These data suggest that inflammation arising from APE1 loss is part of a general disruption of neural homeostasis in the *Ape1*$^{Nes\text{-}cre}$ mutant brain tissue.

Supplementary Figure 5

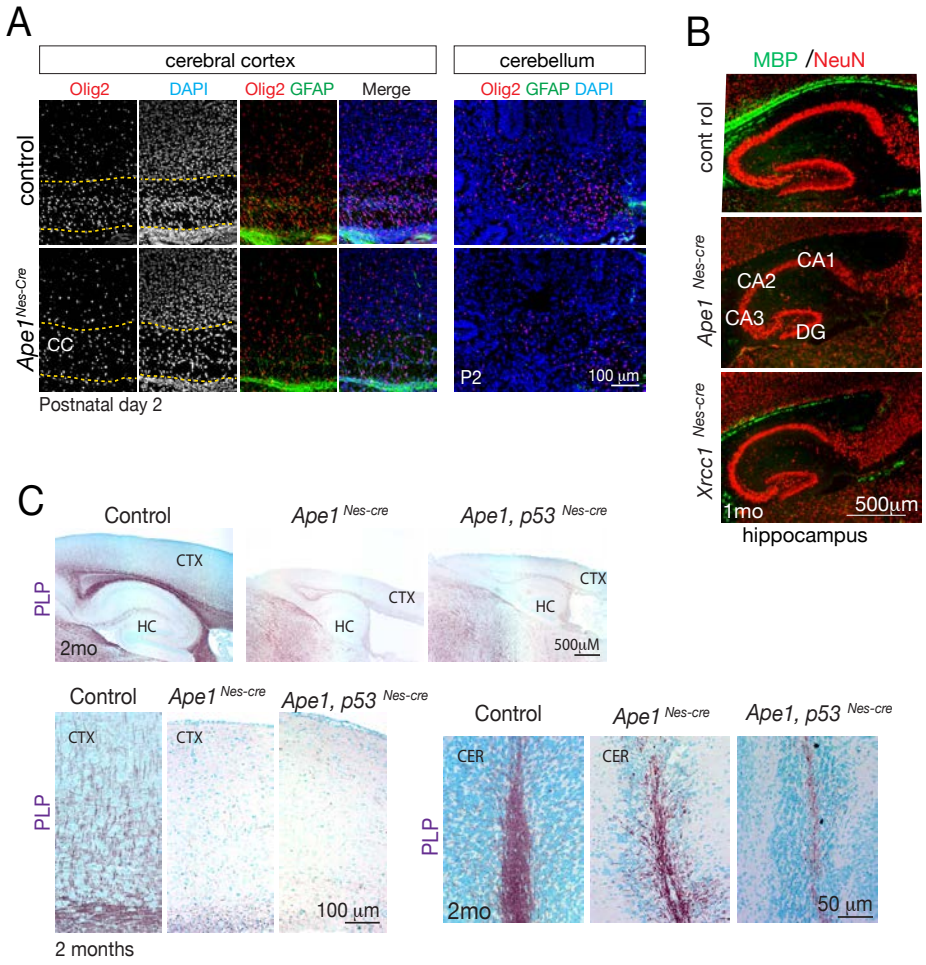

Supplementary Figure 5: Progressive loss of oligodendrocyte results from neural inactivation of APE1.

(A) Olig2 (Oligodendrocyte Transcription Factor 2) is a transcription factor important for progenitor development and labels oligodendrocyte nuclei. Olig 2 immunostaining is reduced in oligodendrocyte precursors by postnatal day 2 in the Ape1 mutant cortex and the white matter region of the cerebellum cerebellum. At

this early stage (P2) in postnatal development, glial fibrillary associated protein (GFAP) does not show increased staining indicating that at this early stage in oligodendrocyte dysfunction that gliosis does not occur. (B) The BER pathway is critical for normal myelination as shown by decreased myelin basic protein (MBP) immunostaining in the corpus callosum of both XRCC1- and APE1-deficient tissues. The hippocampal formation is indicated, which also shows a size reduction due to postnatal cell loss; CA is the cornu ammons and DG is the dentate gyrus. (C) By 2 months of age widespread loss of myelin is apparent in the *Ape1* mutants, and this is independent of p53 status. PLP is proteolipid protein; CTX is the cortex and CER is the cerebellum.

Supplementary Figure 6

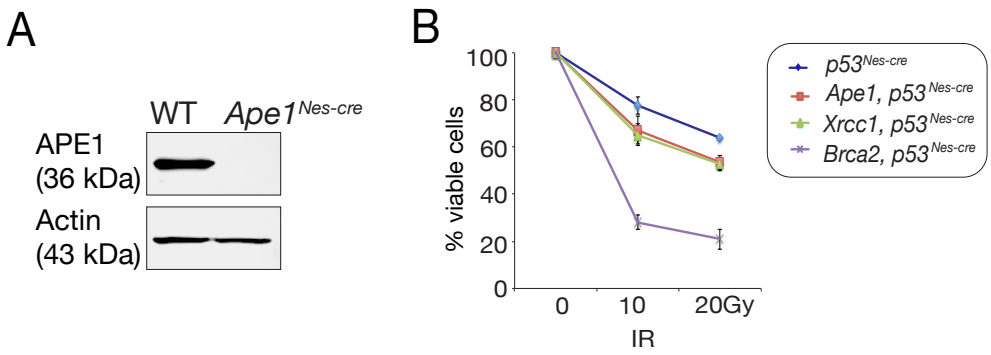

Supplementary Figure 6: APE1 is deleted in *Ape1*$^{Nes\text{-}cre}$ astrocytes and *Atm*$^{-/-}$ cells are mildly sensitive to IR. A. Western blot analysis shows APE1 is undetectable in the *Ape1*$^{Nes\text{-}cre}$-derived primary astrocytes. B. *Ape1*$^{-/-}$ astrocytes are mildly sensitive to ionizing radiation (IR) at indicated doses. *Brac2*$^{-/-}$ cells were hypersensitive to IR compared with either *Ape1*$^{-/-}$ or *Xrcc1*$^{-/-}$ cells.

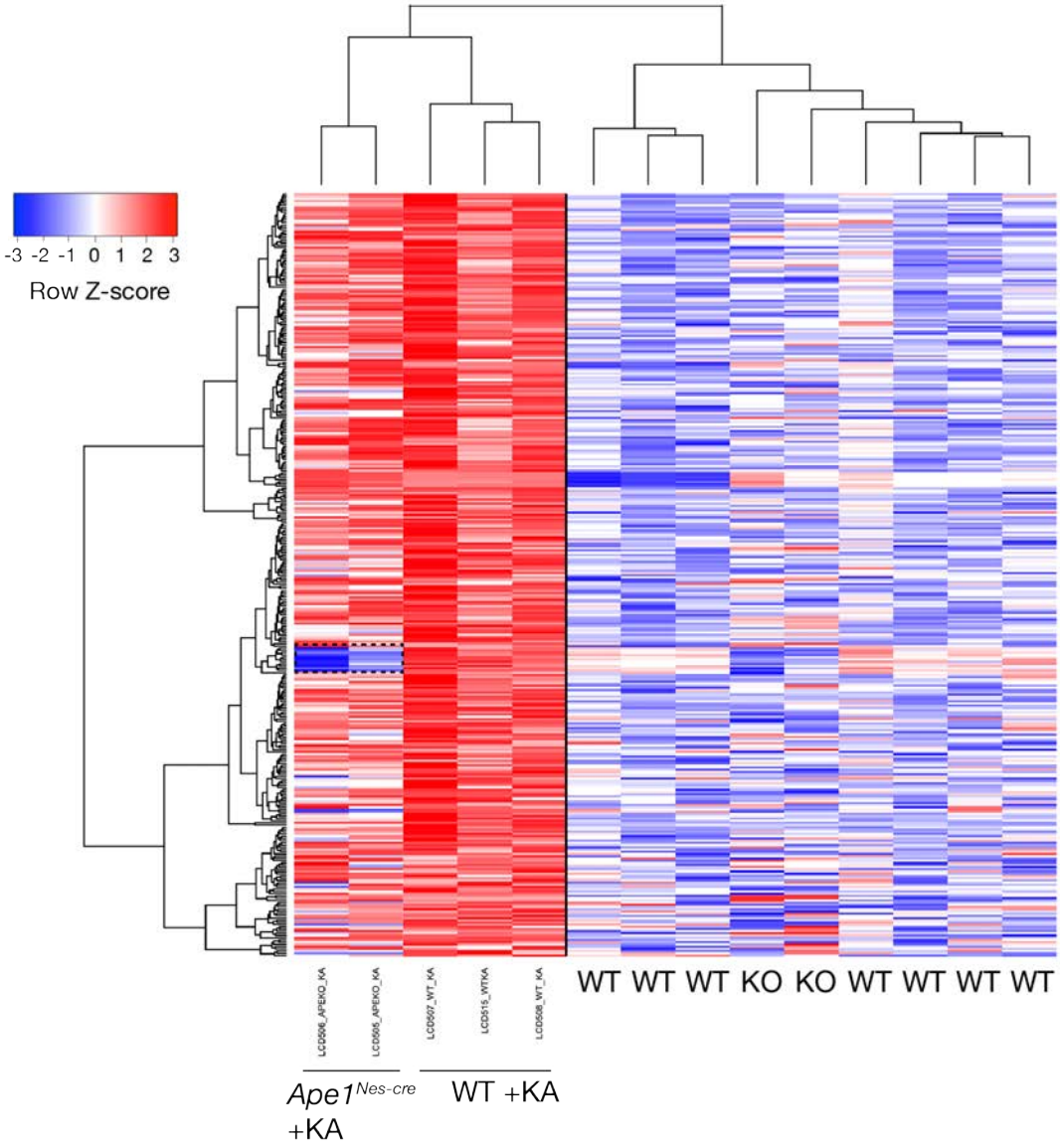

Supplementary Figure 7: Kainic acid treatment results in broad gene expression changes in both WT and *Ape1* mutant hippocampus.

Gene expression in isolated hippocampal tissue was determined using Affymetrix genechips (Mouse Gene 2.0 ST platform). Exposure to kainic acid (KA) resulted in the increased expression of a large number of genes in both control and *Ape1*$^{Nes\text{-}cre}$

tissue. Dendrograms and scaling for rows and columns are shown and calculated based on means. However, compared to the upregulated genes in control tissue, there was a group of in the mutant hippocampus whose expression is not altered by KA; a full list of all gene expression changes that happen after KA is provided in Supplementary Table 1. Not all genes with limited or no expression changes in the *Ape1*$^{Nes\text{-}cre}$ tissue after KA are included in the boxed region shown on the heatmap. References for pathway analysis are: Huang DW, Sherman BT, Lempicki RA. Systematic and integrative analysis of large gene lists using DAVID Bioinformatics Resources. ***Nature Protoc. 2009;4(1):44-57 and*** Huang DW, Sherman BT, Lempicki RA. Bioinformatics enrichment tools: paths toward the comprehensive functional analysis of large gene lists. ***Nucleic Acids Res. 2009;37(1):1-13.***

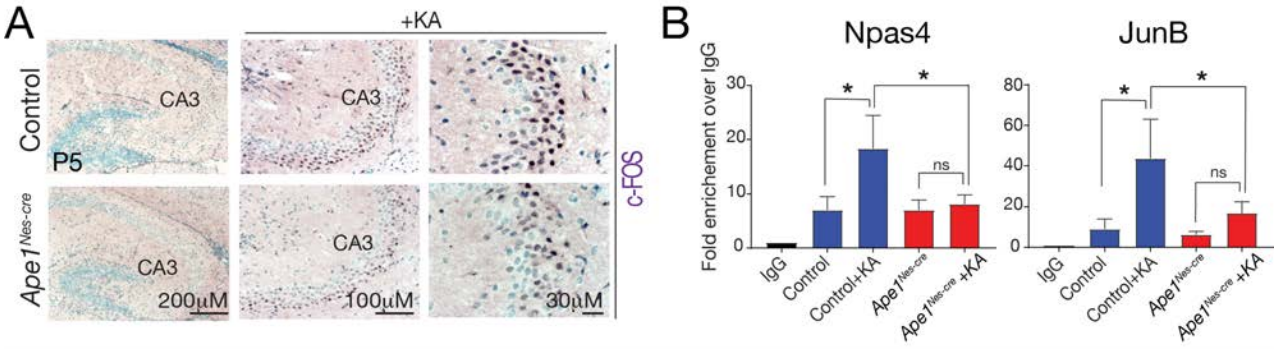

Supplementary Figure 8: AP-1 binding is reduced after KA in APE1Nes-cre hippocampus. A. Activation of c-Fos is markedly reduced throughout the CA3 region of the *Ape1*$^{Nes\text{-}cre}$ hippocampus; arrows). B. ChIP shows KA treatment increases binding of the transcription factor AP1 to the promoter of immediate-early genes *Npas4* or *JunB* in WT hippocampus, while this promoter binding is significantly reduced in *Ape1*$^{Nes\text{-}cre}$ tissue ($p<0.05$).

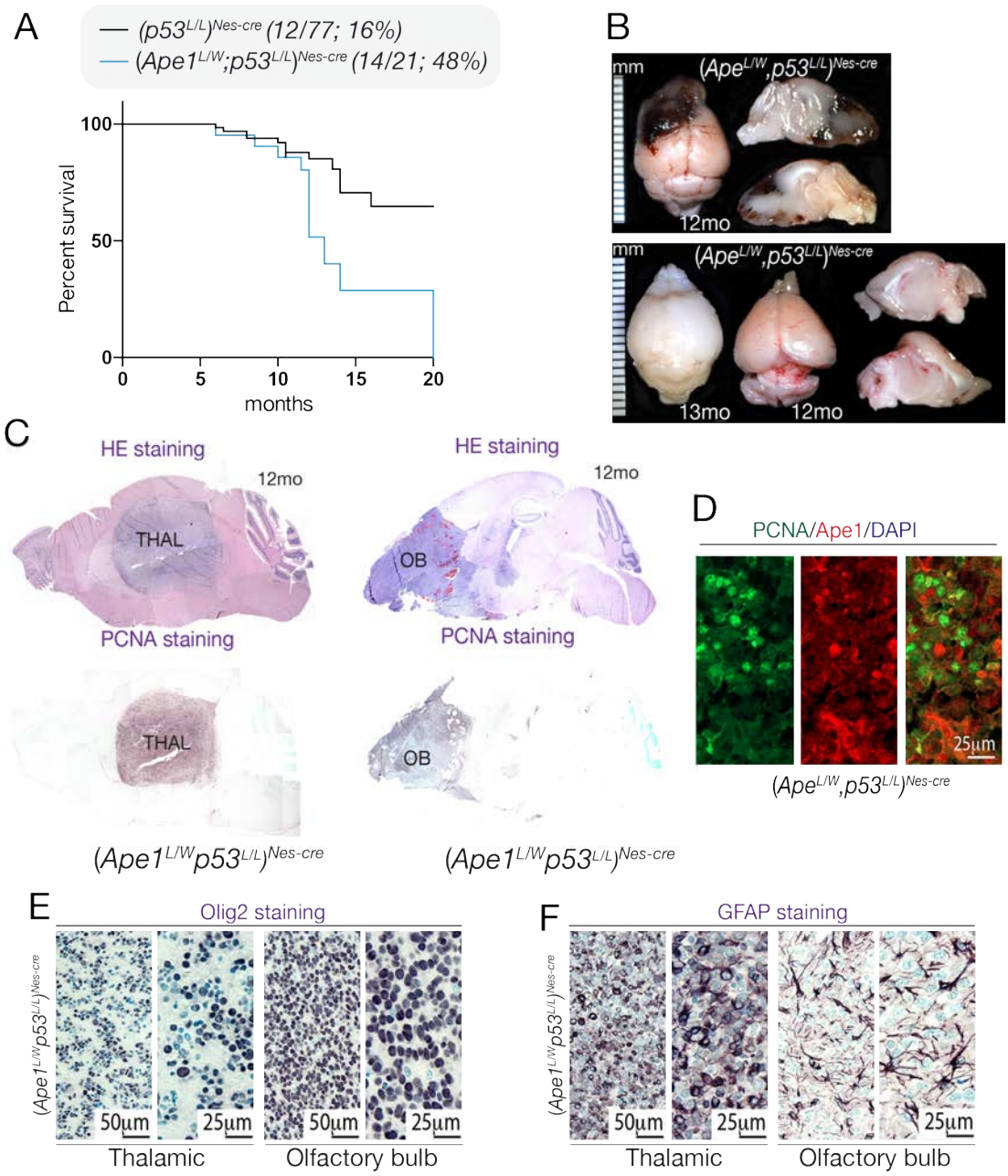

Supplementary Figure 9: *Ape1* heterozygotes primarily develop glioblastoma.

Compared to double knockout mice ($Ape1^{L/L};p53^{L/L}$)$^{Nes\text{-}cre}$, in which both *Ape1* and *p53* are homozygously inactivated, ($Ape1^{+/L};p53^{L/L}$)$^{Nes\text{-}cre}$ mice have an increased latency for tumor development, and ~50% of these animals developed gliomas (A,

B). These gliomas were localized in cortical, thalamic (THAL) and olfactory bulb (OB) regions (C). APE1 immunostaining was absent from the tumors suggesting that the inactivation of the remaining *Ape1* allele was important for tumor formation (D). The gliomas were also often positive for the glial/oligodendrocyte markers Olig2 and GFAP (E, F).

Supplementary Table 1. Functional DAVID Annotation Chart showing top 20 WT downregulated genes

Category	Term	Count	PValue	Genes
INTERPRO	IPR017452:GPCR, rhodopsin-like, 7TM	56	2.41E-15	*VMN1R128, OLFR311, VMN1R127, VMN1R121, OLFR981, VMN1R124, VMN1R120, OLFR1420, OLFR657, OLFR656, GM16451, VMN1R94, OLFR119, VMN1R91, VMN1R118, VMN1R119, VMN1R117, VMN1R116, VMN1R57, VMN1R151, VMN1R114, GPR139, OLFR1307, VMN1R158, VMN1R159, OLFR1383, VMN1R157, OLFR495, OLFR213, OLFR1371, VMN1R143, VMN1R40, OLFR177, VMN1R148, VMN1R149, OLFR172, VMN1R188, OLFR1326-PS1, OLFR1335, OLFR1448, OLFR723, VMN1R3, OLFR632, GM8677, VMN1R132, OLFR1269, CSPRS, GM4201, OLFR606, OLFR916, OLFR8, VMN1R129, VMN1R103, VMN1R104, VMN1R101, VMN1R100*
GOTERM_BP_DIRECT	GO:0050909~sensory perception of taste	14	8.53E-14	*VMN1R128, VMN1R114, VMN1R127, VMN1R132, VMN1R148, VMN1R94, VMN1R121, VMN1R124, VMN1R91, VMN1R120, VMN1R159, VMN1R118, VMN1R157, VMN1R100*
INTERPRO	IPR007960:Mammalian taste receptor	14	2.25E-13	*VMN1R128, VMN1R114, VMN1R127, VMN1R132, VMN1R148, VMN1R94, VMN1R121, VMN1R124, VMN1R91, VMN1R120, VMN1R159, VMN1R118, VMN1R157, VMN1R100*
GOTERM_MF_DIRECT	GO:0016503~pheromone receptor activity	18	4.14E-12	*VMN1R117, VMN1R116, VMN1R143, VMN1R57, VMN1R40, VMN1R151, VMN1R149, VMN1R188, VMN1R158, GM4201, GM16451, VMN1R3, VMN1R129, VMN1R103, GM8677, VMN1R104, VMN1R101, VMN1R119*
INTERPRO	IPR004072:Vomeronasal receptor, type 1	18	1.63E-11	*VMN1R117, VMN1R116, VMN1R143, VMN1R57, VMN1R40, VMN1R151, VMN1R149, VMN1R188, VMN1R158, GM4201, GM16451, VMN1R3, VMN1R129, VMN1R103, GM8677, VMN1R104, VMN1R101, VMN1R119*
GOTERM_MF_DIRECT	GO:0004930~G-protein coupled receptor activity	47	1.80E-11	*OLFR1371, VMN1R128, OLFR311, VMN2R41, VMN2R42, VMN1R127, OLFR177, VMN1R40, VMN2R90, VMN1R148, VMN1R121, VMN1R124, OLFR981, OLFR172, VMN1R120, OLFR1326-PS1, OLFR1420, VMN2R47, VMN2R48, VMN2R45, OLFR657, OLFR1335, OLFR1448, OLFR656, VMN1R94, OLFR723, OLFR632, VMN2R-PS104, OLFR119, VMN1R91, VMN1R118, GPR139, VMN1R114, VMN1R132, OLFR1307, VMN2R36, VMN1R159, VMN2R38, OLFR1383, VMN1R157, OLFR1269, OLFR606, OLFR916, OLFR8, OLFR495, OLFR213, VMN1R100*
INTERPRO	IPR002971:Major urinary protein	9	1.13E-10	*MUP10, MUP7, MUP1, MUP3, MUP2, MUP8, MUP13, MUP12, MUP11*
SMART	SM00349:KRAB	18	3.13E-10	*GM14308, 5730507C01RIK, GM14444, GM14434, GM14296, GM14295, GM14412, GM14403, GM14440, GM14327, ZFP951, ZFP781, GM14391, GM14393, GM14322, GM10324, GM11009, GM14305*
GOTERM_MF_DIRECT	GO:0036094~small molecule binding	9	3.48E-10	*MUP10, MUP7, MUP1, MUP3, MUP2, MUP8, MUP13, MUP12, MUP11*
INTERPRO	IPR002345:Lipocalin	9	5.45E-10	*MUP10, MUP7, MUP1, MUP3, MUP2, MUP8, MUP13, MUP12, MUP11*
INTERPRO	IPR022272:Lipocalin conserved site	9	1.57E-09	*MUP10, MUP7, MUP1, MUP3, MUP2, MUP8, MUP13, MUP12, MUP11*
INTERPRO	IPR000566:Lipocalin/cytosolic fatty-acid binding protein domain	10	1.59E-08	*MUP10, MUP7, RBP1, MUP1, MUP3, MUP2, MUP8, MUP13, MUP12, MUP11*
INTERPRO	IPR012674:Calycin	10	3.98E-08	*MUP10, MUP7, RBP1, MUP1, MUP3, MUP2, MUP8, MUP13, MUP12, MUP11*
INTERPRO	IPR011038:Calycin-like	10	4.51E-08	*MUP10, MUP7, RBP1, MUP1, MUP3, MUP2, MUP8, MUP13, MUP12, MUP11*
INTERPRO	IPR001909:Krueppel-associated box	18	2.16E-07	*GM14308, 5730507C01RIK, GM14444, GM14434, GM14296, GM14295, GM14412, GM14403, GM14440, GM14327, ZFP951, ZFP781, GM14391, GM14393, GM14322, GM10324, GM11009, GM14305*
GOTERM_MF_DIRECT	GO:0005550~pheromone binding	10	7.32E-07	*MUP10, MUP7, MUP1, MUP3, MUP2, VMN1R188, MUP8, MUP13, MUP12, MUP11*
GOTERM_BP_DIRECT	GO:0071396~cellular response to lipid	5	4.27E-06	*MUP1, MUP3, MUP2, MUP12, MUP11*
GOTERM_BP_DIRECT	GO:0031649~heat generation	5	4.27E-06	*MUP1, MUP3, MUP2, MUP12, MUP11*
GOTERM_BP_DIRECT	GO:0045834~positive regulation of lipid metabolic process	5	4.27E-06	*MUP1, MUP3, MUP2, MUP12, MUP11*
GOTERM_MF_DIRECT	GO:0005009~insulin-activated receptor activity	5	4.46E-06	*MUP1, MUP3, MUP2, MUP12, MUP11*